FLUKA Applications to Neutrino Beams

Workshop on Neutrino Beams and Instrumentation

Fermilab, 6-9 september 2000

A. Ferrari, P.R Sala

CERN (on leave from INFN-Milan)

Topics

- General description of FLUKA
- General description of Hadron-Nucleus (h-A) interactions
  - The low/intermediate energy hN model
  - The high energy hN model
  - The low/intermediate energy hA model
  - The high energy hA model
- Particle Decay
- Selected topics and benchmarks
  - The SPY data and WANF
  - Complex benchmarks
- Applications of FLUKA interaction models to ν simulations
  - Neutrino-nucleus interactions and NOMAD
  - The atmospheric neutrino calculations
  - CNGS

FLUKA

Authors: **A. Fassò[†], A. Ferrari[&], J. Ranft[*], P.R. Sala[&]**
[†] SLAC , [&] INFN Milan and CERN, [*] Siegen University

Interaction and transport MonteCarlo code.

- Hadron-hadron and hadron-nucleus interactions 0-20 TeV
- Nucleus-nucleus interactions 0-10000 TeV/n: *under development !!!*
- Electromagnetic and μ interactions 0-100 TeV
- Charged particle transport - ionization energy loss
- Neutron multigroup transport and interactions 0-20 MeV
- Analogue or biased calculations

A multipurpose code

The program can be used in different fields such as shielding, dosimetry, high energy experimental physics and engineering, cosmic ray studies, medical physics, etc.

- Each radiation component is treated as far as possible with the same level of accuracy (it's like having 4 different programs in one, for pure neutron, electron-photon or muon problems – and hadrons, of course!)
- FLUKA can be run in fully analog mode, for calorimetry. It can calculate coincidences and anticoincidences
- It can also be run in biased mode, for shielding design

  But also experimental high energy physicists need sometimes to make studies of deep penetration or rare events: hadron punchthrough, radiation background in underground experiments, muon production over short decay lengths

The FLUKA hadron-nucleon interaction models

Elastic, charge exchange and strangeness exchange reactions based on available phase-shift analysis and/or fits of experimental double-differential data. At high energies, standard eikonal approximations are used.

Particle production interactions: two models:

- The "resonance" one, which covers the energy range up to 3–5 GeV
- The high energy one, based on the Dual Parton Model, which provides reliable results up to several tens of TeV

Nonelastic hN interactions at intermediate energies

- $N_1 + N_2 \rightarrow N_1' + N_2' + \pi$ threshold around 290 MeV, important above 700 MeV,
- $\pi + N \rightarrow \pi' + \pi'' + N'$ opens at 170 MeV.

Dominance of the Δ resonance and of the N^* resonances $\rightarrow$ reactions treated in the framework of the isobar model $\rightarrow$ all reactions proceed through an intermediate state containing at least one resonance.

$$
\begin{aligned}
N_1 + N_2 &\rightarrow N_1' + \Delta(1232) \rightarrow N_1' + N_2' + \pi \\
\pi + N &\rightarrow \Delta(1600) \rightarrow \pi' + \Delta(1232) \rightarrow \pi' + \pi'' + N' \\
N_1 + N_2 &\rightarrow \Delta_1(1232) + \Delta_2(1232) \rightarrow N_1' + \pi_1 + N_2' + \pi_2
\end{aligned}
$$

Resonance energies, widths, cross sections, branching ratios from data and conservation laws, whenever possible. Inferred from inclusive cross sections when needed

inelastic hN at high energies: DPM

- Problem: "soft" interactions $\rightarrow$ no perturbation theory.
- Solution : Interacting strings (quarks held together by the gluon-gluon interaction into the form of a string)
- Interactions treated in the Reggeon-Pomeron framework
- At sufficiently high energies the leading term corresponds to a Pomeron (IP) exchange (a closed string exchange)
- each colliding hadron splits into two colored partons $\rightarrow$ combination into two color neutral chains $\rightarrow$ two back-to-back jets
- Physical particle exchange produce single chains at low energies
- higher order contributions with multi-Pomeron exchanges important at $E_{lab} \geq$ 1 TeV

DPM: chain examples

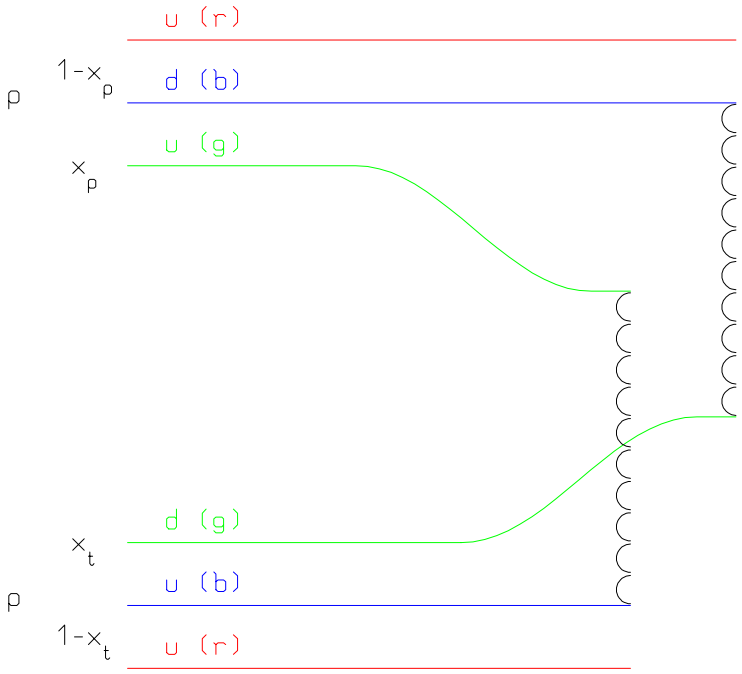

Leading two-chain diagram in DPM for $p - p$ scattering. The color (red, blue, and green) and quark combination shown in the figure is just one of the allowed possibilities

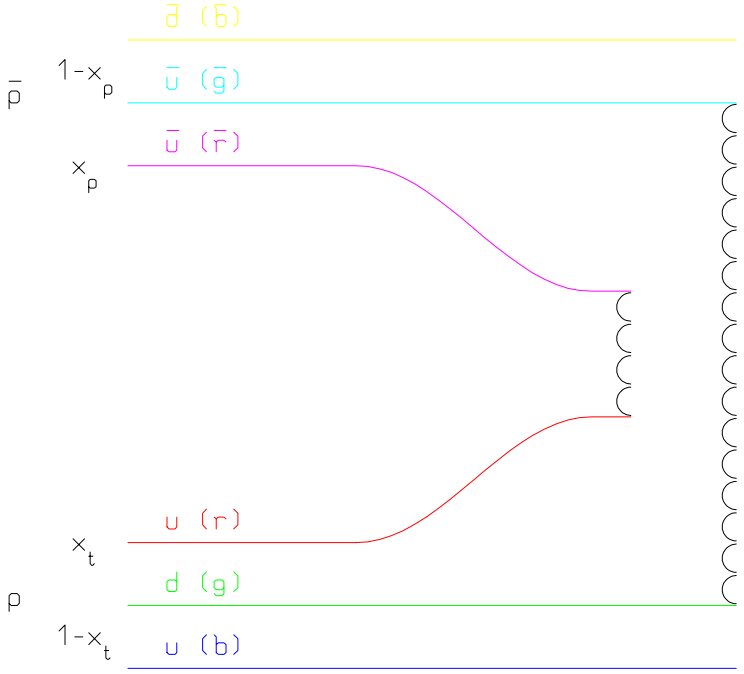

Leading two-chain diagram in DPM for $\bar{p} - p$ scattering. The color (red, blue, and green) and quark combination shown in the figure is just one of the allowed possibilities

DPM: chain examples II

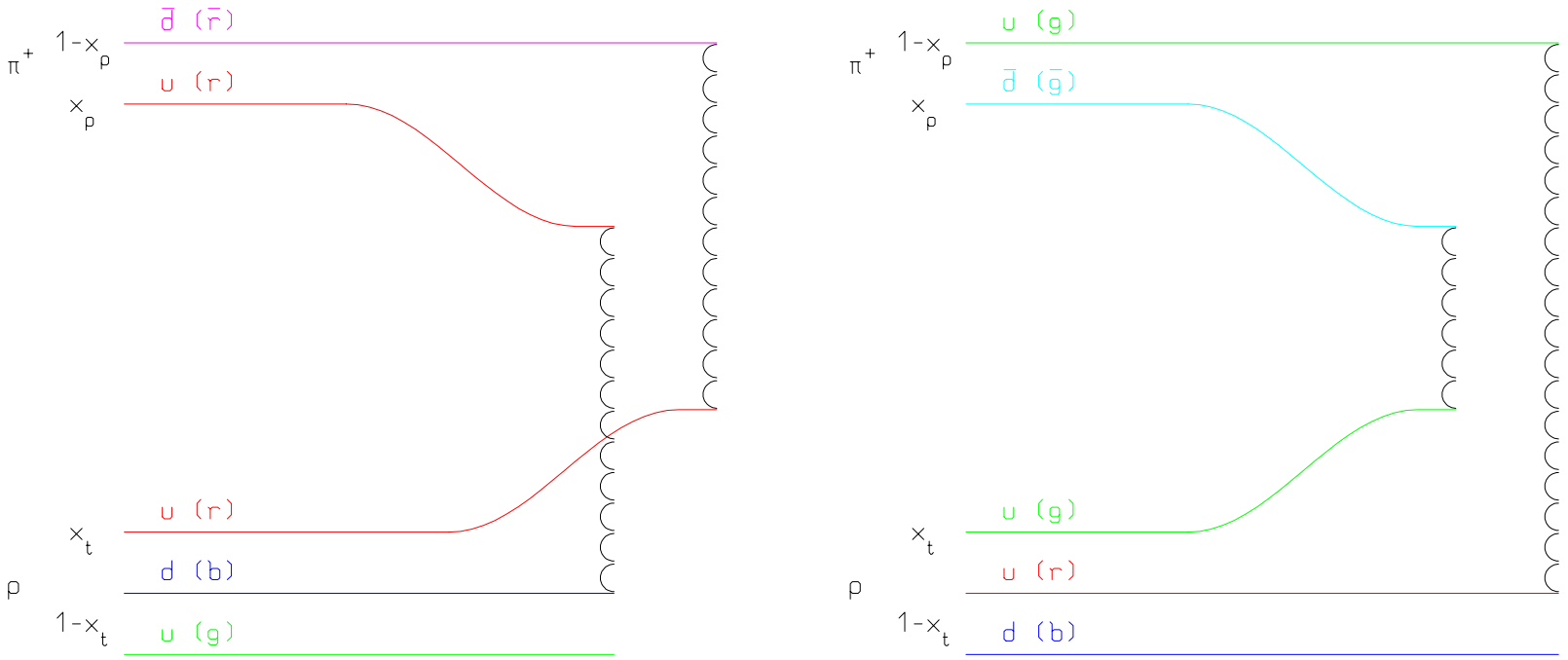

Leading two-chain diagrams in DPM for $\pi^+ - p$ scattering. The color (red, blue, and green) and quark combination shown in each figure is just one of the allowed possibilities

DPM and fragmentation

from DPM:

- Number of chains
- Chain composition
- Chain energies and momenta
- Diffractive events

Almost No Freedom

Chain hadronization

- Assumes chain universality
- Fragmentation functions from hard processes and e^+e^-
- Transverse momentum from e^{-bm_T} behaviour
- Mass effects at low energies

The same functions and (few) parameters for all reactions and energies

Nonelastic hN at high E :(π^+ p), 7-22 GeV

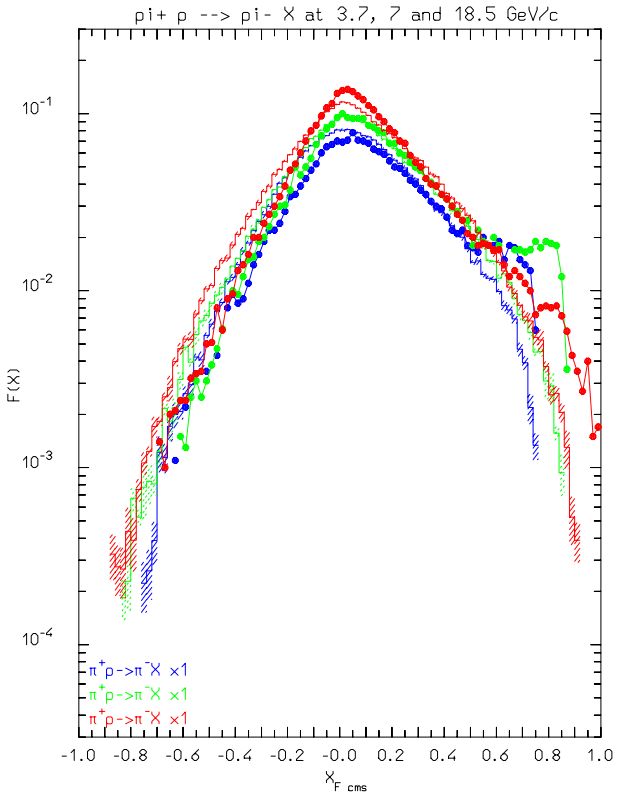

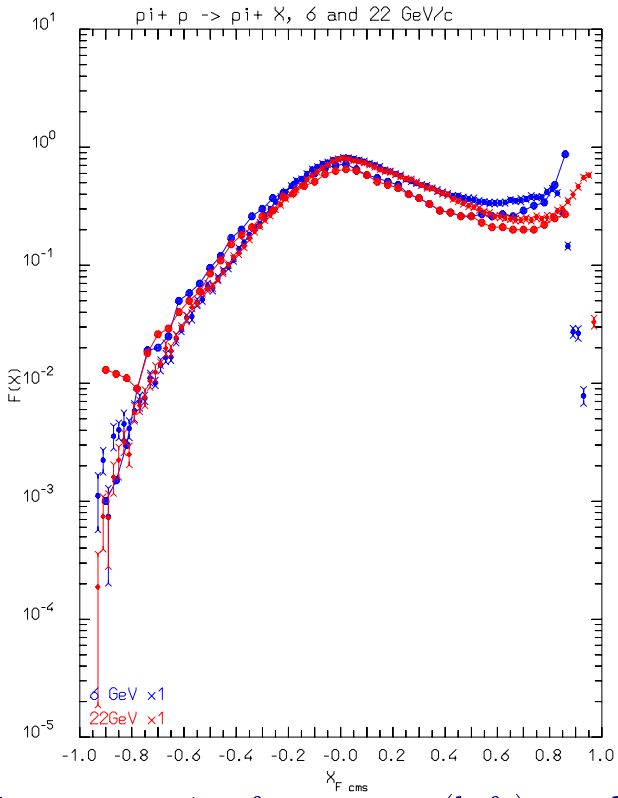

Invariant cross section spectra, as a function of Feynman x_F^* of negative (left), and positive (right) pions emitted for π^+ on protons at various momenta. Data from M.E Law et al. LBL80 (1972).

Nonelastic hN high E: (K^-p) , (π^-p) 10-16 GeV, p_T

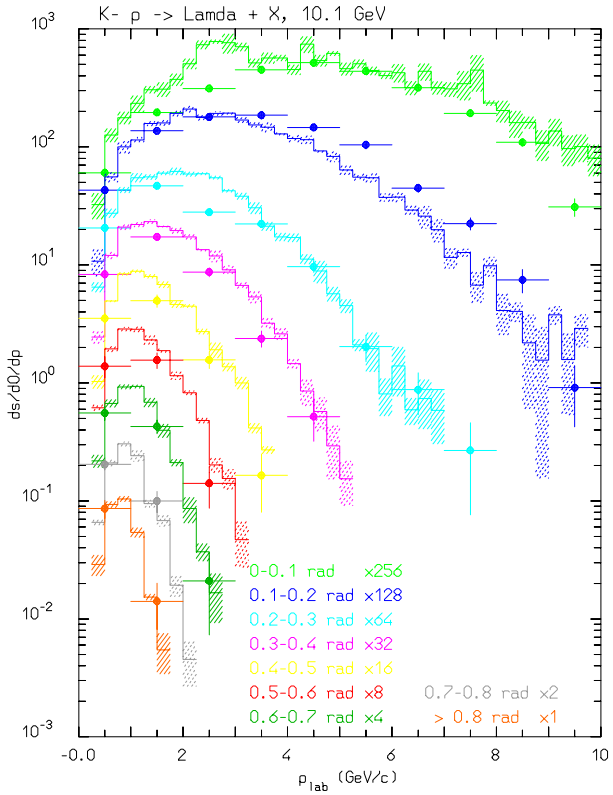

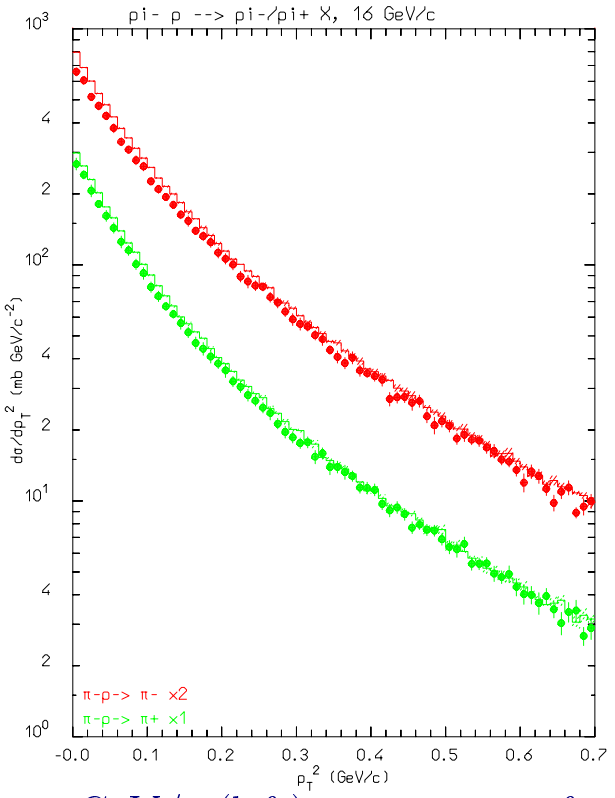

Double differential cross section for $K^-p \to \Lambda X$ at 10 GeV/c (left), p_T spectra of π^+ and π^- produced by 16 GeV/c π^- incident on an hydrogen target. Data from M.E Law et al. LBL80 (1972).

Nonelastic hN high E: (π^+ p) 250GeV, x_F and p_t

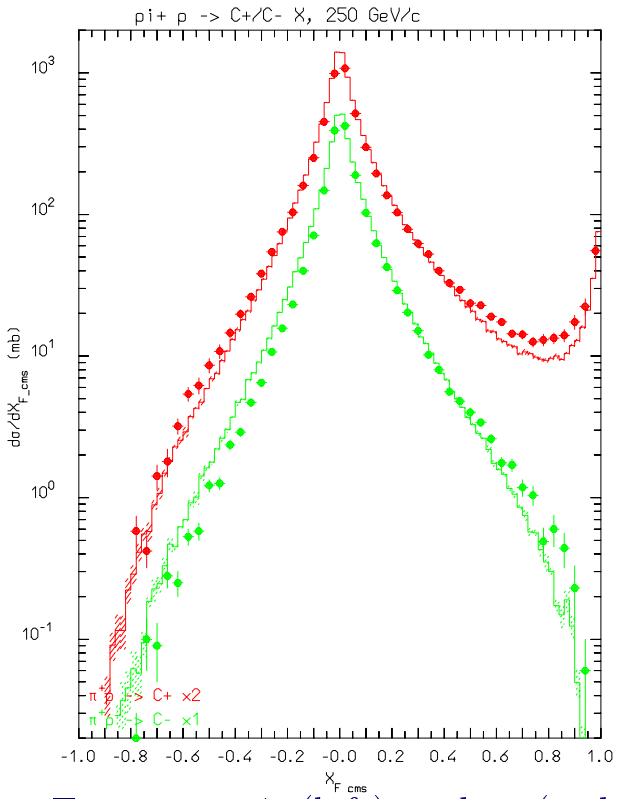

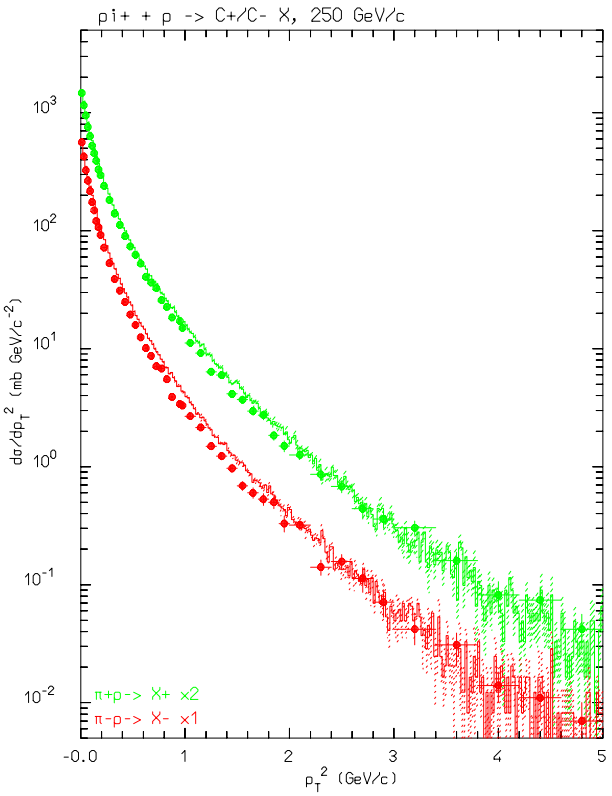

Feynman x_F^* (left) and p_t (right) spectra of positive particles and π^- produced by 250 GeV/c π^+ incident on an hydrogen target. Exp. data (symbols) have been taken from M. Adamus et al. ZPC39, 311 (1988).

The FLUKAhadron-nucleus interaction models

Two models in FLUKA to describe hadron-nucleus nonelastic interactions

- The "low/intermediate" energy one, PEANUT, which covers the energy range up to 4–5 GeV
- The high energy one which can be used up to several tens of TeV

The nuclear physics embedded in the two models is very much the same. The main differences are a coarser nuclear description (and no preequilibrium stage), and the addition of the Gribov-Glauber cascade for the high energy one.

PEANUT is a three step model:

1. (Generalized) IntraNuclear Cascade
2. Preequilibrium
3. Evaporation/Fission or Fermi break-up

and the high energy generator is also a three step model:

1. Gribov-Glauber multiple primary interactions
2. (Generalized) IntraNuclear Cascade
3. Evaporation/Fission or Fermi break-up

(Generalized) IntraNuclear Cascade basic assumptions

1. Primary and secondary particles moving in the nuclear medium
2. Interaction probability from σ_{free} + Fermi motion $\times$ $\rho(r)$ + exceptions (ex. π)
3. Glauber cascade at high energies
4. Classical trajectories $(+)$ nuclear mean potential (resonant for π's!!)
5. Curvature from nuclear potential $\rightarrow$ refraction and reflection.
6. Interactions are incoherent and uncorrelated
7. Interactions in projectile–target nucleon CMS $\rightarrow$ Lorentz boosts
8. Multibody absorption for π, μ^-, K^-
9. Quantum effects (Pauli, formation zone, correlations...)
10. Exact conservation of energy, momenta and all additive quantum numbers, including nuclear recoil

Quantistic effects in (G)INC

1. Pauli blocking,
2. Formation time (inelastic),
3. Coherence length ((quasi)-elastic and charge exchange),
4. Nucleon antisymmetrization,
5. Hard core nucleon correlations

Pion interactions in nuclei

The description of pion interactions on nuclei in the sub-GeV energy range must take into account:

- The resonant nature of the $\pi - N$ interaction, mostly dominated by the $\Delta(1232)$.
- The effect of the nuclear medium on the $\pi - N$ interaction
- The possibility of absorption (both s-wave and p-wave) on two or more nucleons
- The resonant nature of the pion-nucleus potential, which is rapidly varying with the pion energy

Positive Kaons : a probe for Fermi momentum distribution

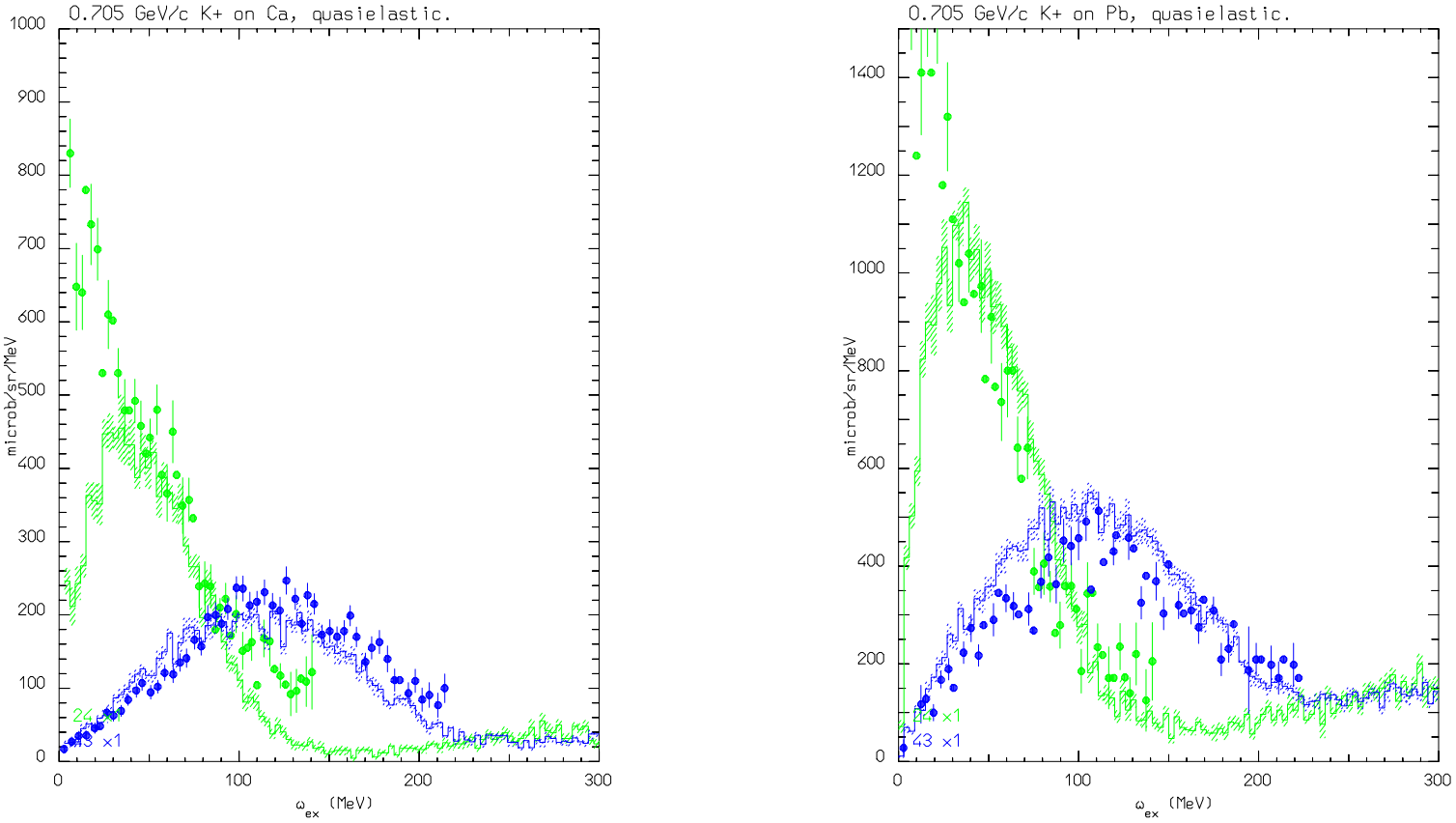

QuasiElastic K^+ Scattering on Ca(left) and Pb(right) vs residual excitation, at 24° and 43°. Histo:FLUKA, dots : data (C.M.Kormanyos et al,Phys. Rev. C51, 669 (1995))

Nonelastic interactions at intermediate energies: examples

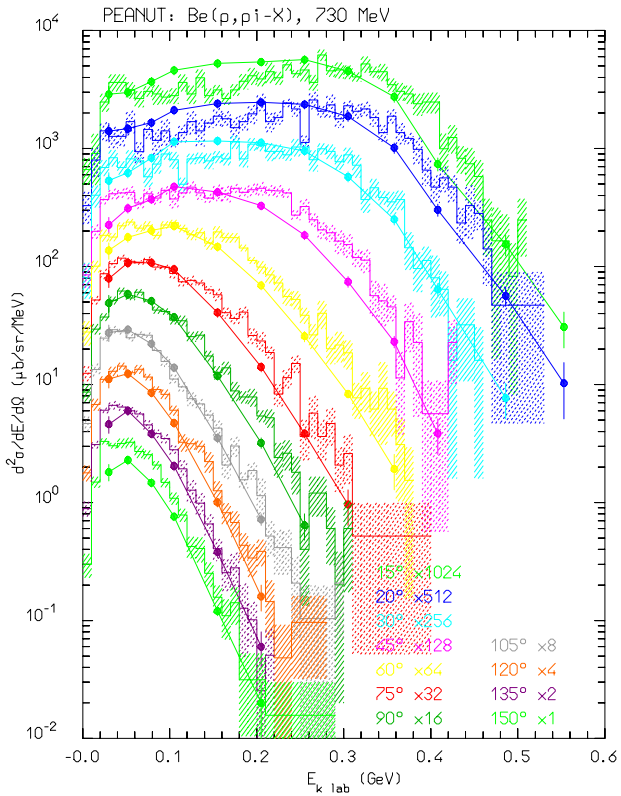

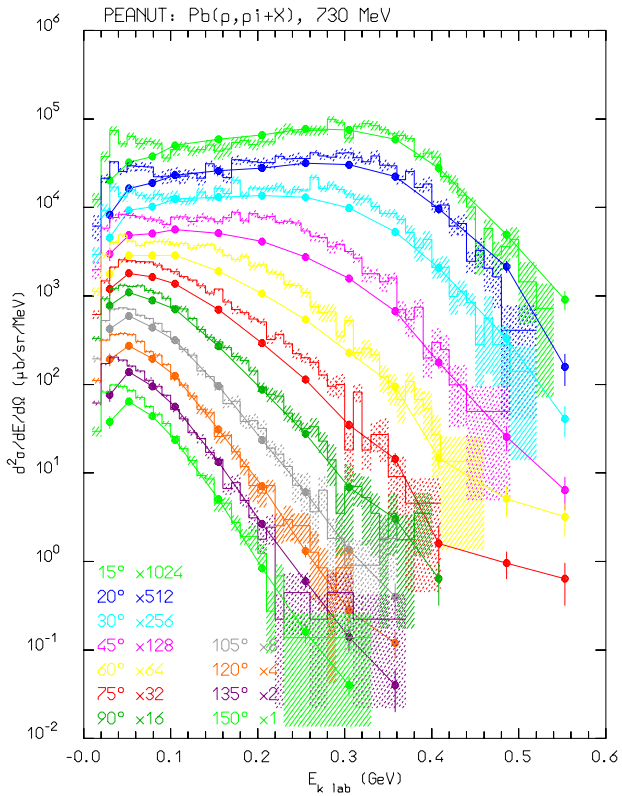

Double differential distributions of π produced by 730 MeV protons. π^-'s from Be (left) and π^+ from Pb (right). Exp.data (symbols) from D.R.F. Cochran et al., **PRD6**,(1972)

hA at high energies: GLAUBER Cascade

Elastic, Quasi-elastic and Absorption hA cross sections derived from Free hadron-Nucleon cross section + Nuclear ground state ONLY .

Inelastic interaction $\equiv$ multiple interaction with ν target nucleons, with binomial distribution:

$$P_{r\ \nu}(b) \equiv \left(\begin{array}{c} A \\ \nu \end{array} \right) P_r^{\nu}(b) \left[1 - P_r(b)\right]^{A-\nu}$$

where $P_r(b) \equiv \sigma_{hN\ r} T_r(b)$, and $T_r(b)$=folding of nuclear density and scattering profiles along the path.

On average :

$$< \nu >= \frac{Z\sigma_{hp\ r} + N\sigma_{hn\ r}}{\sigma_{hA\ abs}} \qquad (1)$$

$$\sigma_{hA\ abs}(s) \ = \ \int \mathrm{d}^2\vec{b} \left[1 - \left(1 - \sigma_{hN\ r}(s) T_r(b)\right)^A\right]$$

hA at high energies: GRIBOV-GLAUBER

Gribov-Glauber= DPM modelling of Multiple Collisions

Interaction with ν target nucleons $\rightarrow 2\nu$ chains

2 chains from projectile valence quarks,

$2(\nu - 1)$ chains from sea $q - \bar{q}$.

No freedom, except in the treatment of mass effects at low energies.

Fermi motion included $\rightarrow$ smearing of p_T distributions

INC follows

Nonelastic hA interactions at high energies: examples

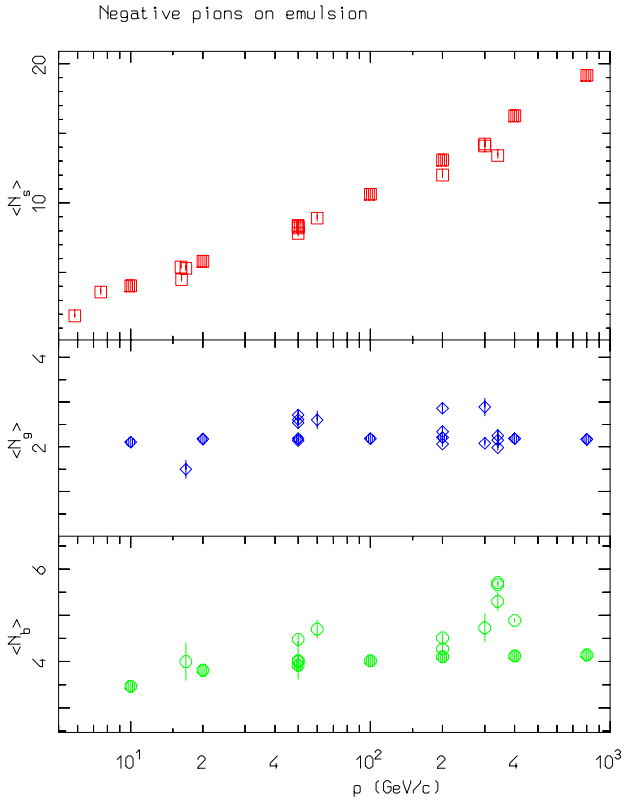

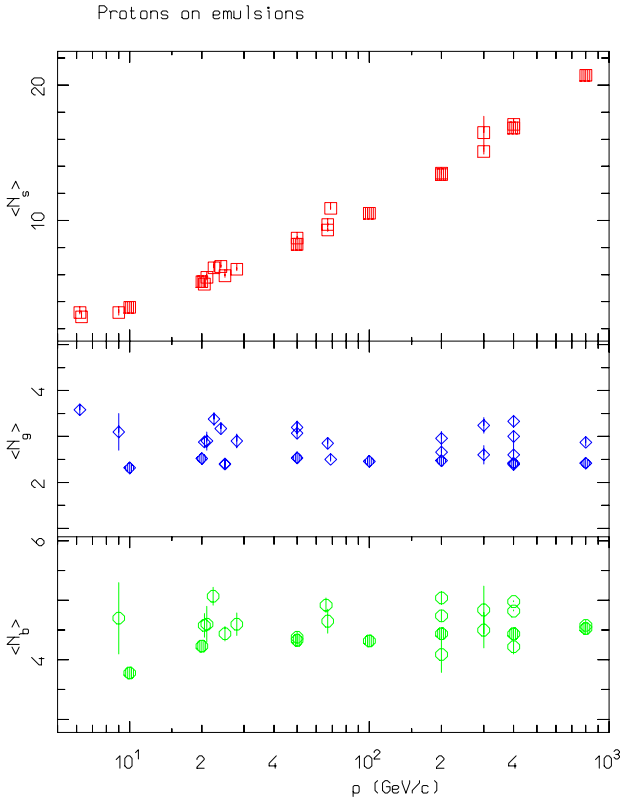

Shower, grey, and black tracks multiplicities for π^- (left) and p (right) on emulsion, as a function of projectile momentum. Open symbols: experimental data from various sources, full symbols :FLUKA results.

Nonelastic hA at high E: (p,Be), 14-24 GeV

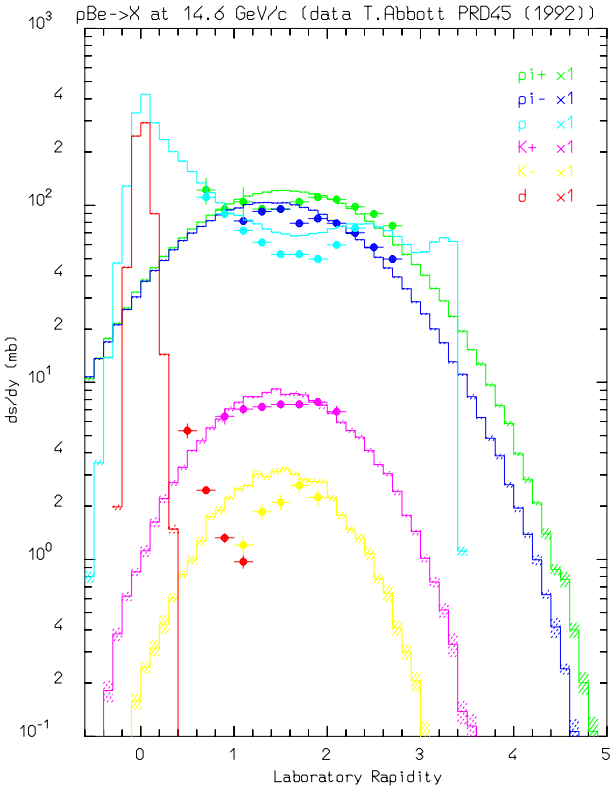

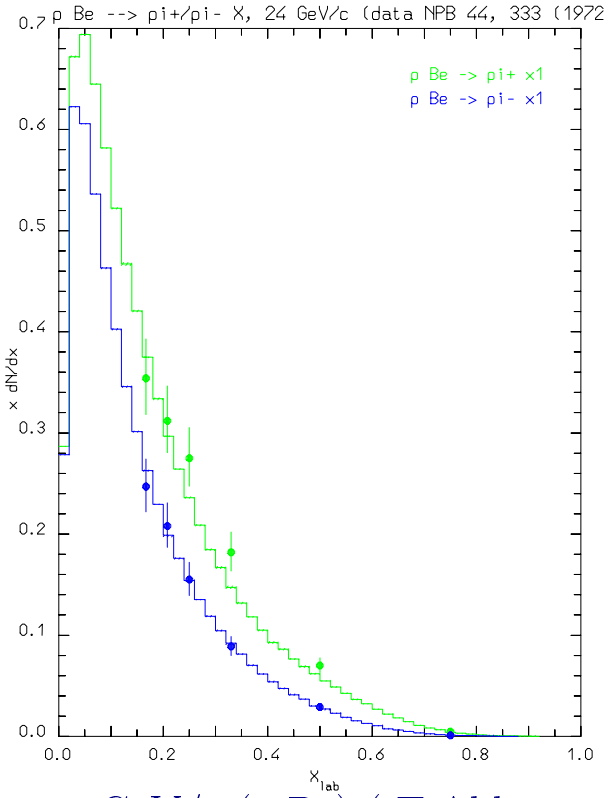

Left: rapidity distribution of $\pi^{+/-}$, $K^{+/-}$, p and d, 14.6 GeV/c (p,Be) (T.Abbott et al PRD45(11), 3906 (1992)). Right: X_{lab} distribution for $\pi^{+/-}$, 24 GeV/c (p,Be) (symbols extrapolated from the DDCS in T.Eichten et al. NPB 44, 333 (1972)).

Nonelastic hA interactions at high energies: examples IV

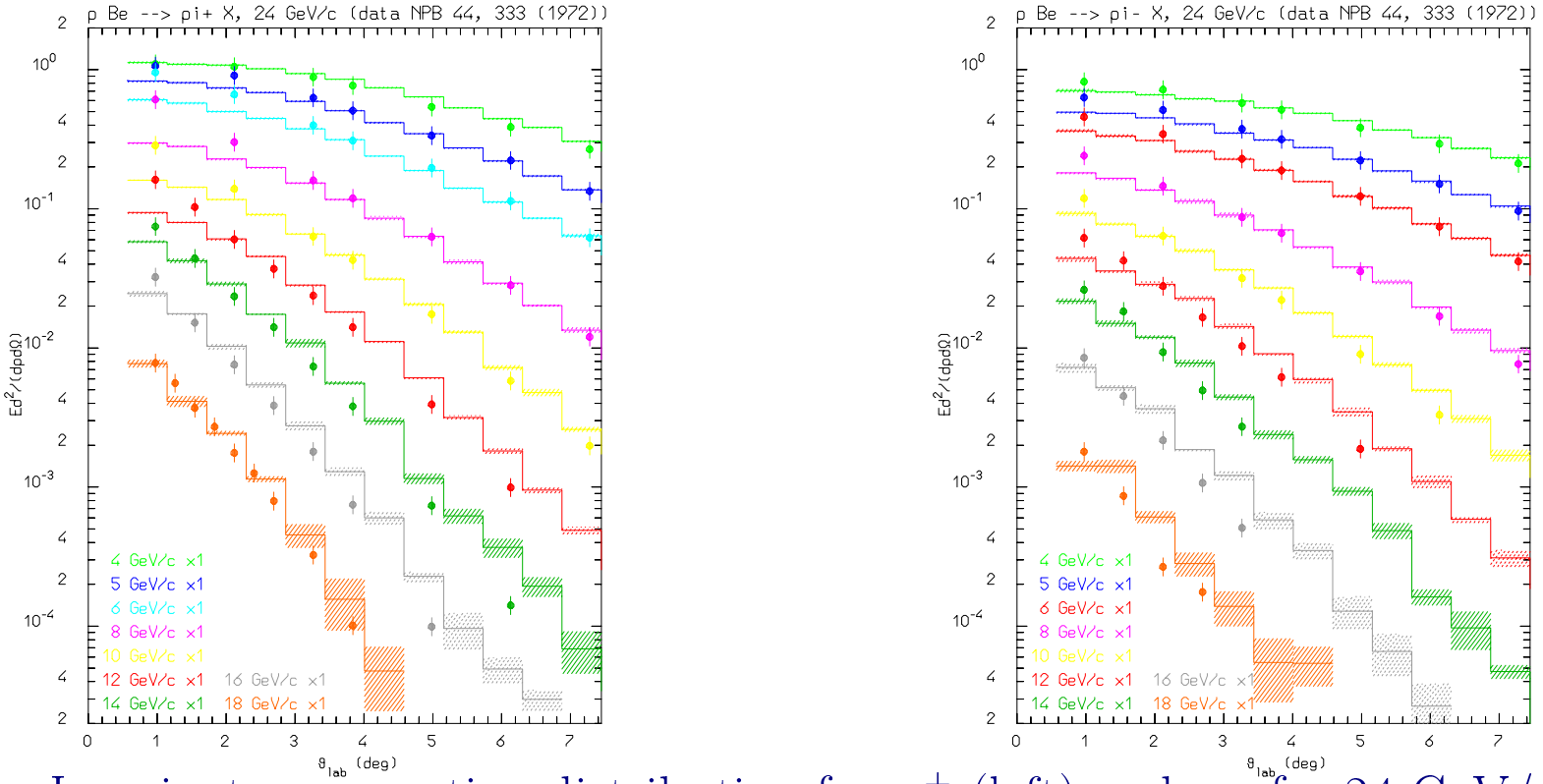

Invariant cross section distribution for π^+ (left) and π^- for 24 GeV/c protons on Be (data from T.Eichten et al. NPB 44, 333 (1972)).

Nonelastic hA interactions at high energies: examples V

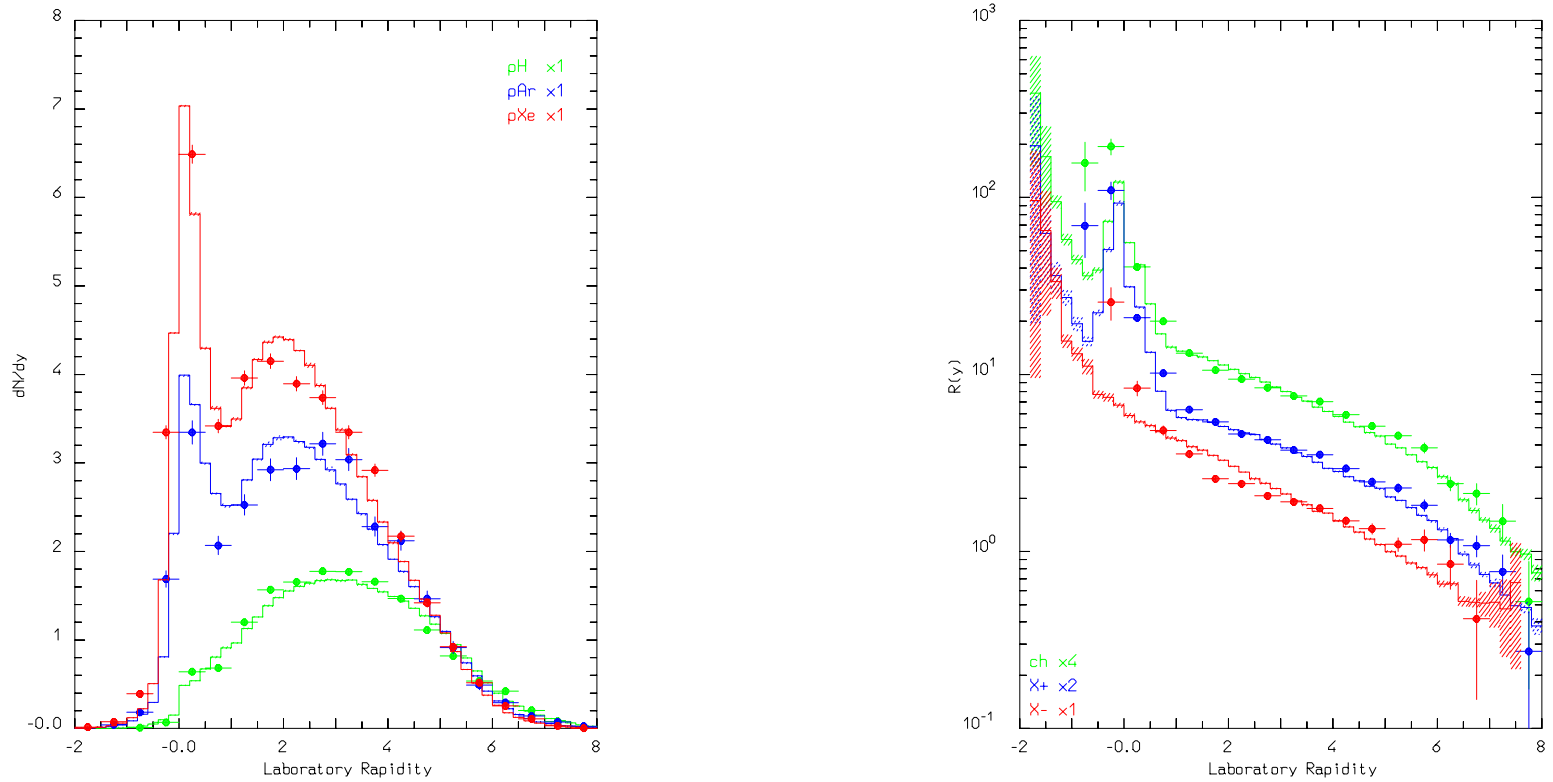

Rapidity distribution of charged particles produced in 200 GeV proton collisions on Hydrogen, Argon, and Xenon target (left) and ratio of rapidity distribution of charged, positive, and negative particles produced in 200 GeV proton collisions on Xenon and Hydrogen (right). Data from C. De Marzo et al., PRD26, 1019 (1982).

Nonelastic hA interactions at high energies: examples VI

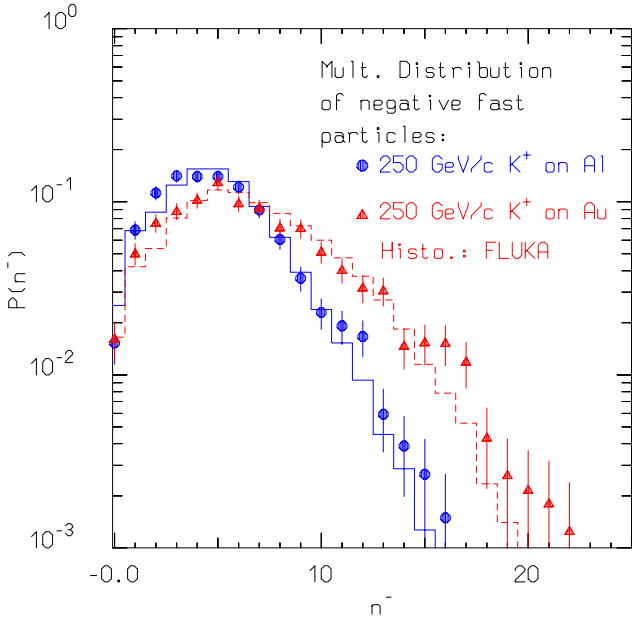

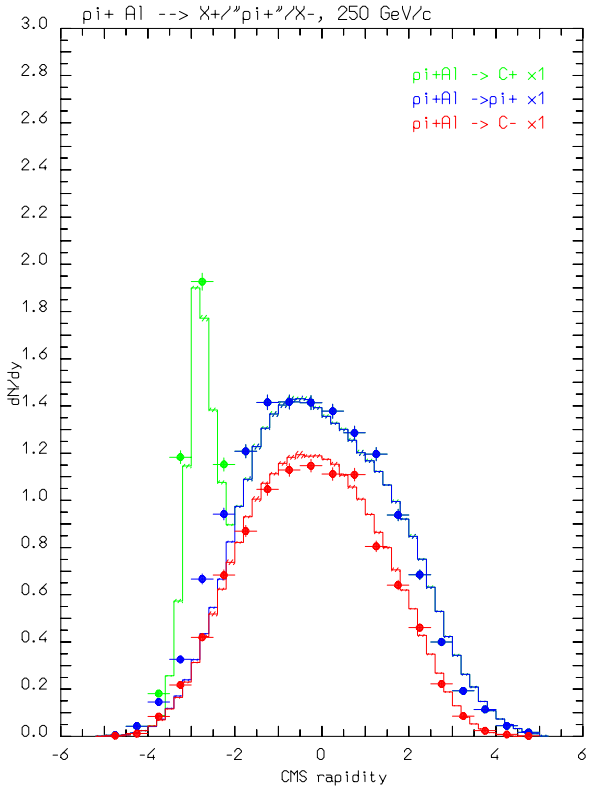

Multiplicity distribution of negative shower particles for 250 GeV/c K^+ on Aluminium and Gold targets (left), and rapidity distribution of positive, negative, and "π^+" particle for 250 GeV/c π^+ on Aluminium (right). Data from I.V. Ajinenko et al. ZPC42 377 (1989) and N.M. Agababyan et al. ZPC50 361 (1991).

Nonelastic hA interactions at high energies: examples VII

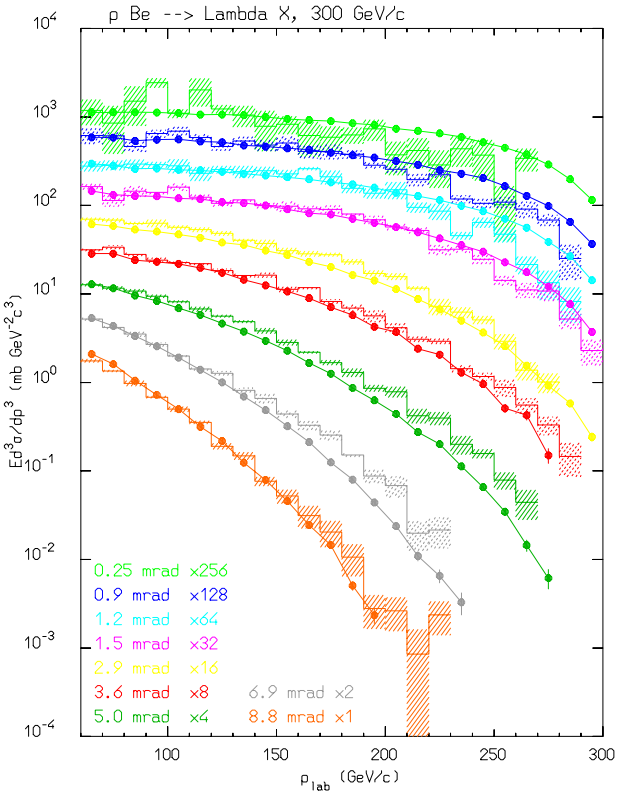

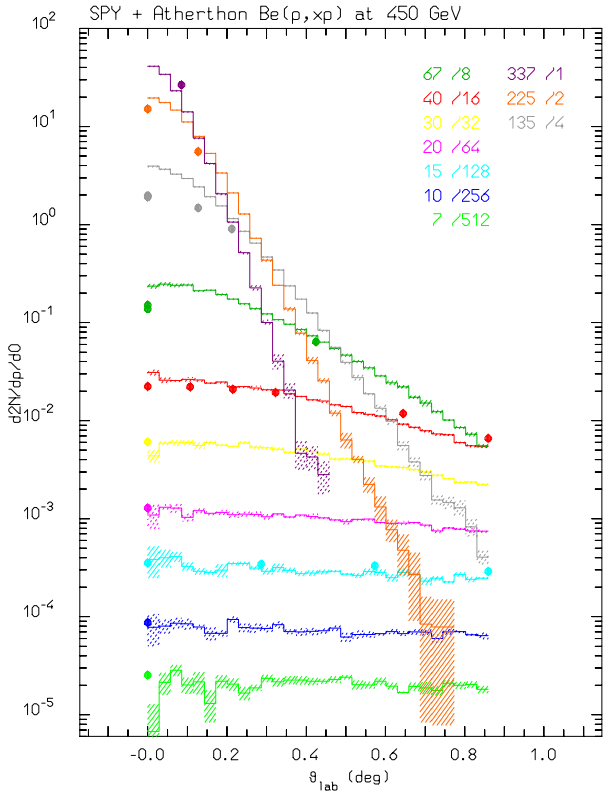

Invariant cross section for Λ production from 300 GeV protons on Be (left, data from P. Skubic et al. PRD 18 3115 (1978)), and double differential cross section for proton production (right) for 450 GeV/c protons on a 10 cm thick Be target (data from H.W. Atherton CERN 80–07, G. Ambrosini et al. PL B425 208 (1988)).

hA interactions at high E: Energy scaling

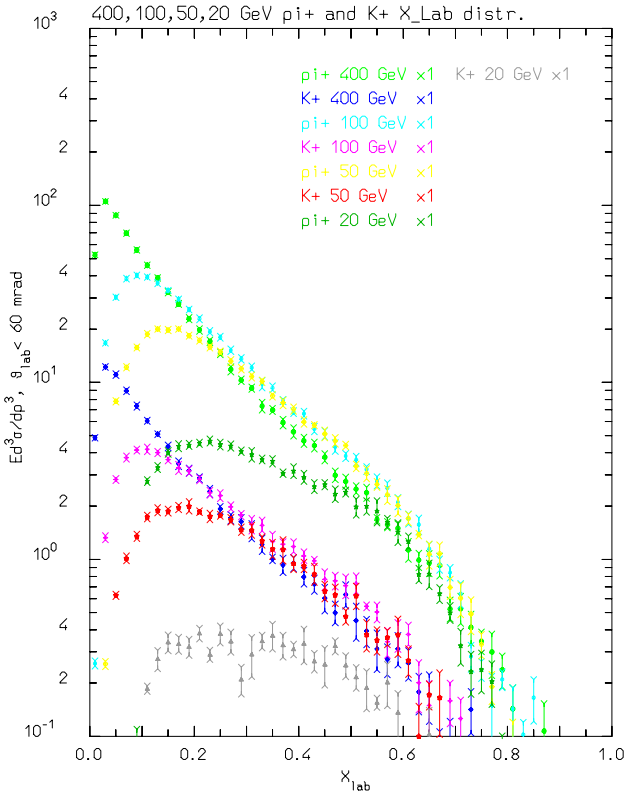

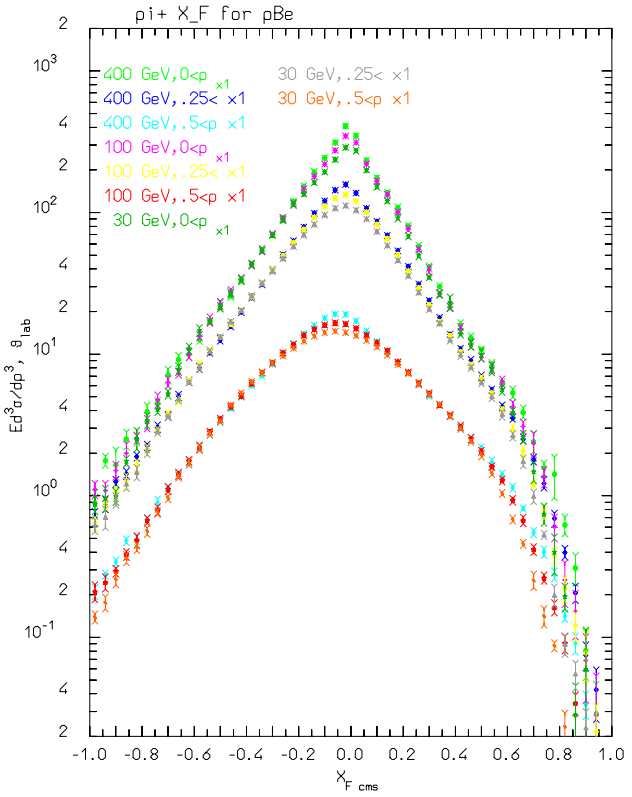

LEFT: X_{lab} distribution of π^+ and K^+ from p on CNGS target

RIGHT: X_{cms} distribution of π^+ in different p_T bins from (p,Be) (thin target) at different energies

hA interactions at high E: different projectiles

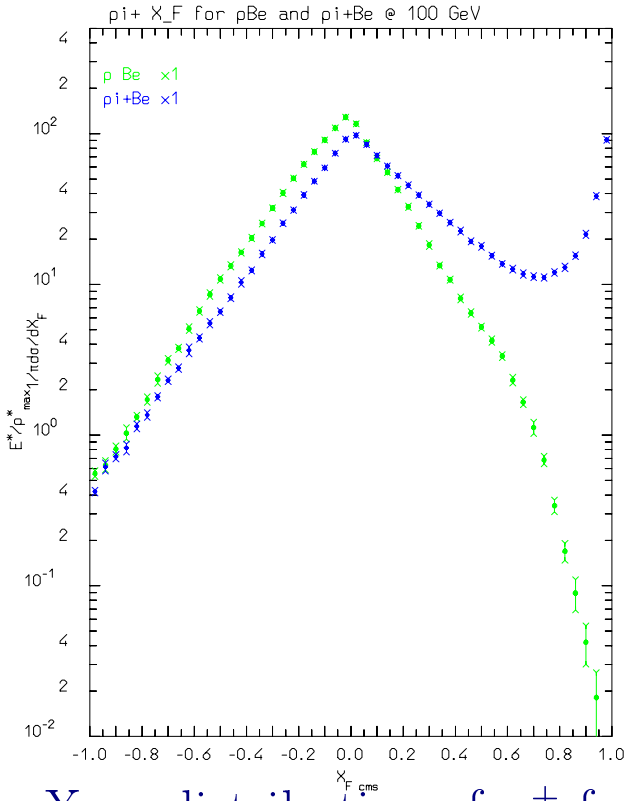

σ(p,Be)=195 mb
$\sigma(\pi^+$,Be)=145 mb
$< \nu >$(p,Be)=1.4
$< \nu >(\pi^+$,Be)=1.2

X_{cms} distribution of π^+ from (p,Be) and (π^+,Be) (thin target) at 100 GeV

hA interactions at high E: different targets

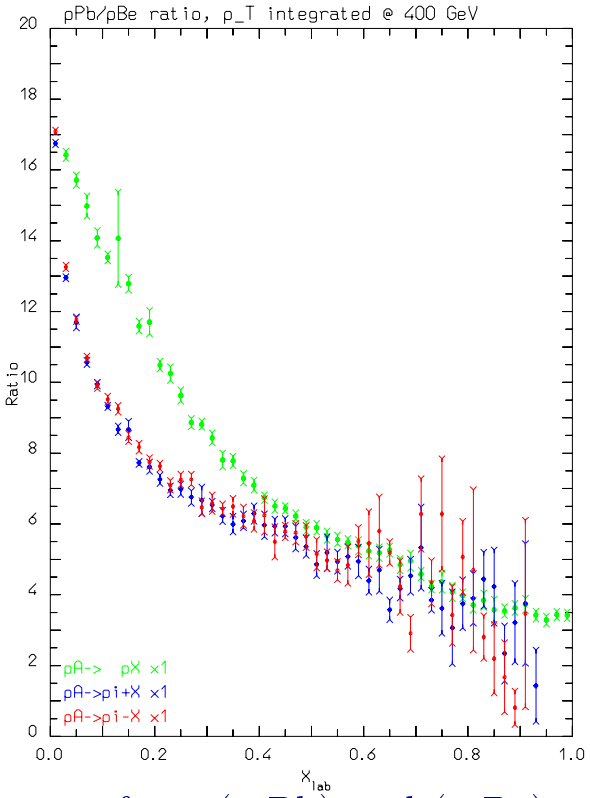

Ratio of invariant cross sections from (p,Pb) and (p,Be) at 400 GeV, as a function of X. The three curves refer to produced protons, π^+ and π^-, p_T integrated.

Particle decay

- two-body π and K : phase space , μ polarization
- $K_{\mu 3}$ and K_{e3} : Matrix elements from V. Patera , KLOE collaboration
- μ Proper V-A matrix element, full account for polarization
- Biasing procedures for decay length and decay direction

Recent improvements in the high energy model

G. Collazuol, A. Ferrari, A. Guglielmi and P.R. Sala, NIM A 449 (2000), 609

The DPM + Glauber model embedded into old FLUKAversions (and in *GEANT-FLUKA*) had important limitations:

- Glauber cascade described at an elementary level;
- all resonances assumed on mass shell;
- coarse chain hadronization, and no particular attention to threshold and finite mass effects;
- isospin conservation not enforced at each individual hadron production step;
- transverse motion reasonable but still far from satisfactory;
- simplified description of diffractive processes.

Recent improvements in the high energy model

All improved along the years. Most critical point: chain hadronization

- Threshold and finite mass effects checked against low energy data (chains with 2 or 3 had.)
- Fragmentation functions checked against 16-450 GeV h-N and h-A data
- Constraint: hadron multiplicity at 200 GeV.
- Balanced optimization: better SPY agreement could be achieved, spoiling low energy data.

Improvements: SPY I : forward yield

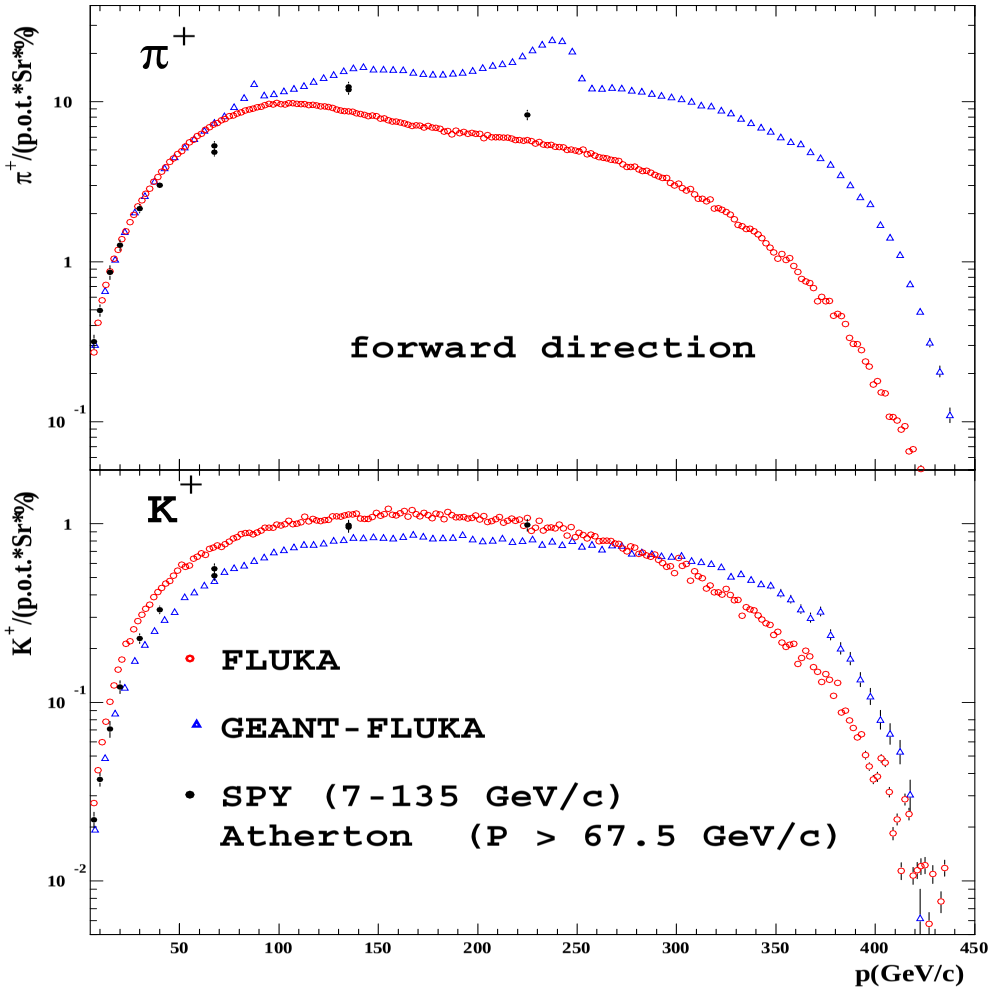

π^+ and K^+

$d^2N\,/\,(dp/p\,d\Omega)$

100 mm Be target,

$\theta \leq 0.2$ mrad

SPY ($P \leq 135$ GeV/c, •)

and Atherton et al.

($P \geq 67.5$ GeV/c,)

compared with the

FLUKA and the

GEANT-FLUKA

predictions.

Improvements: SPY II : forward yield

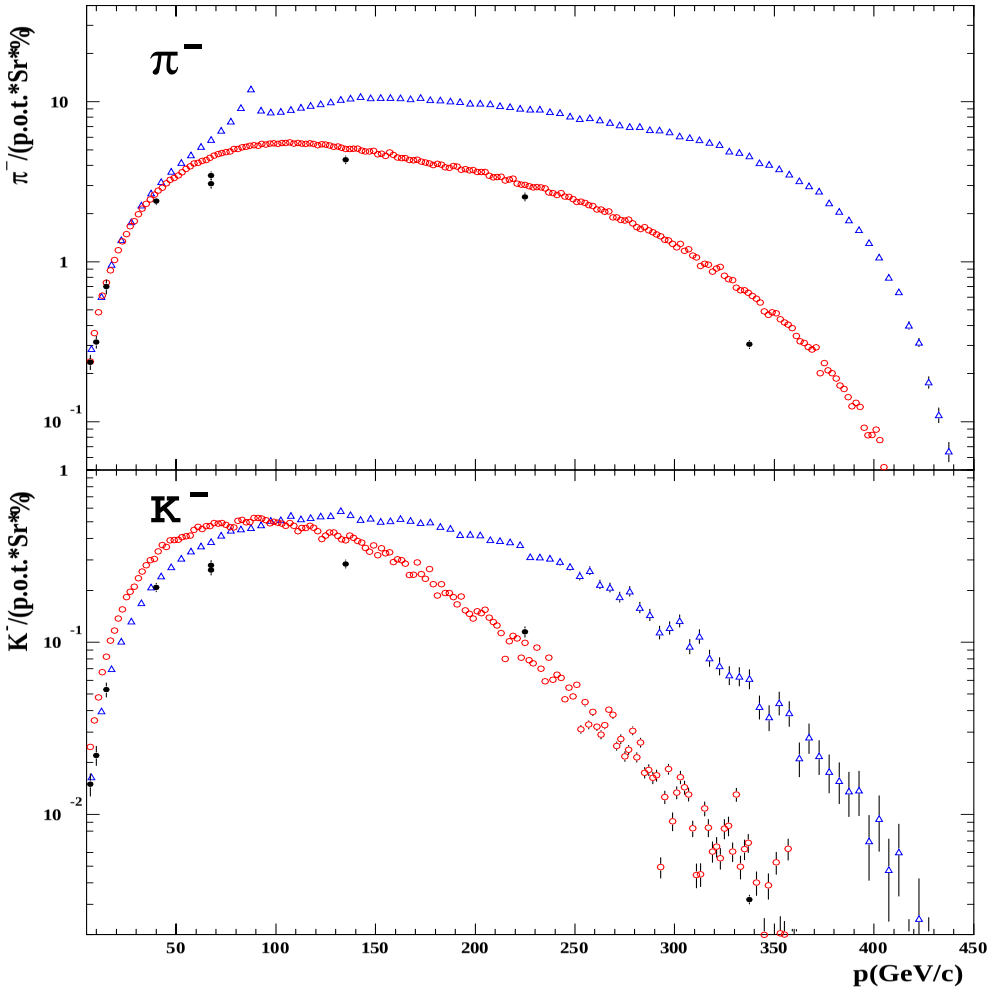

π^- and K^-

$d^2N\,/\,(dp/p\,d\Omega)$

100 mm Be target,

$\theta \leq 0.2$ mrad

SPY ($P \leq 135$ GeV/c, •)

and Atherton et al.

($P \geq 67.5$ GeV/c,)

compared with the

FLUKA and the

GEANT-FLUKA

predictions.

Comparison with SPY I

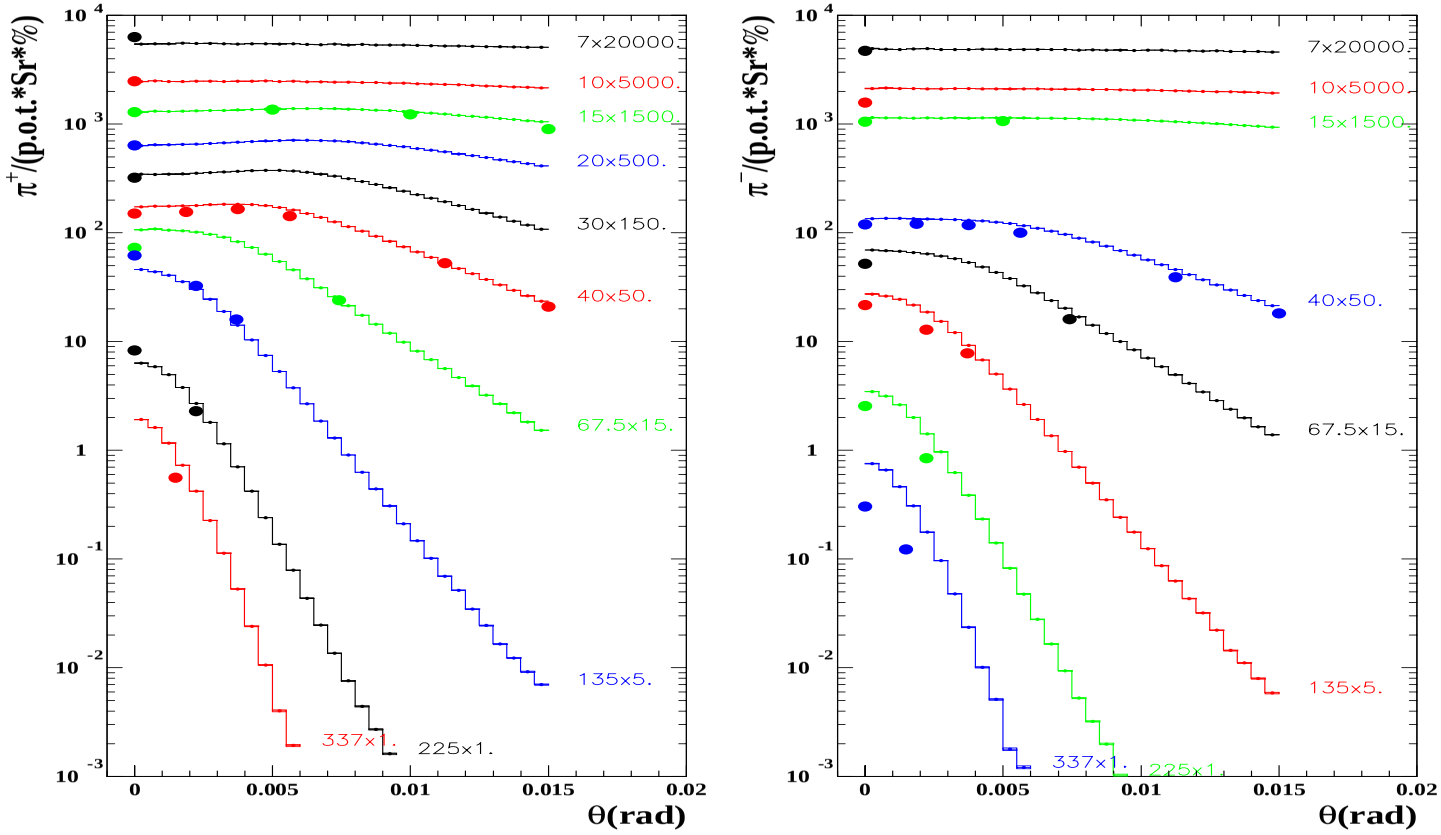

Double differential cross section for π^+ (left) and π^- (right) production for 450 GeV/c protons on a 10 cm thick Be target (data from H.W. Atherton CERN 80–07, G. Ambrosini et al. PL B425 208 (1988)).

Comparison with SPY II

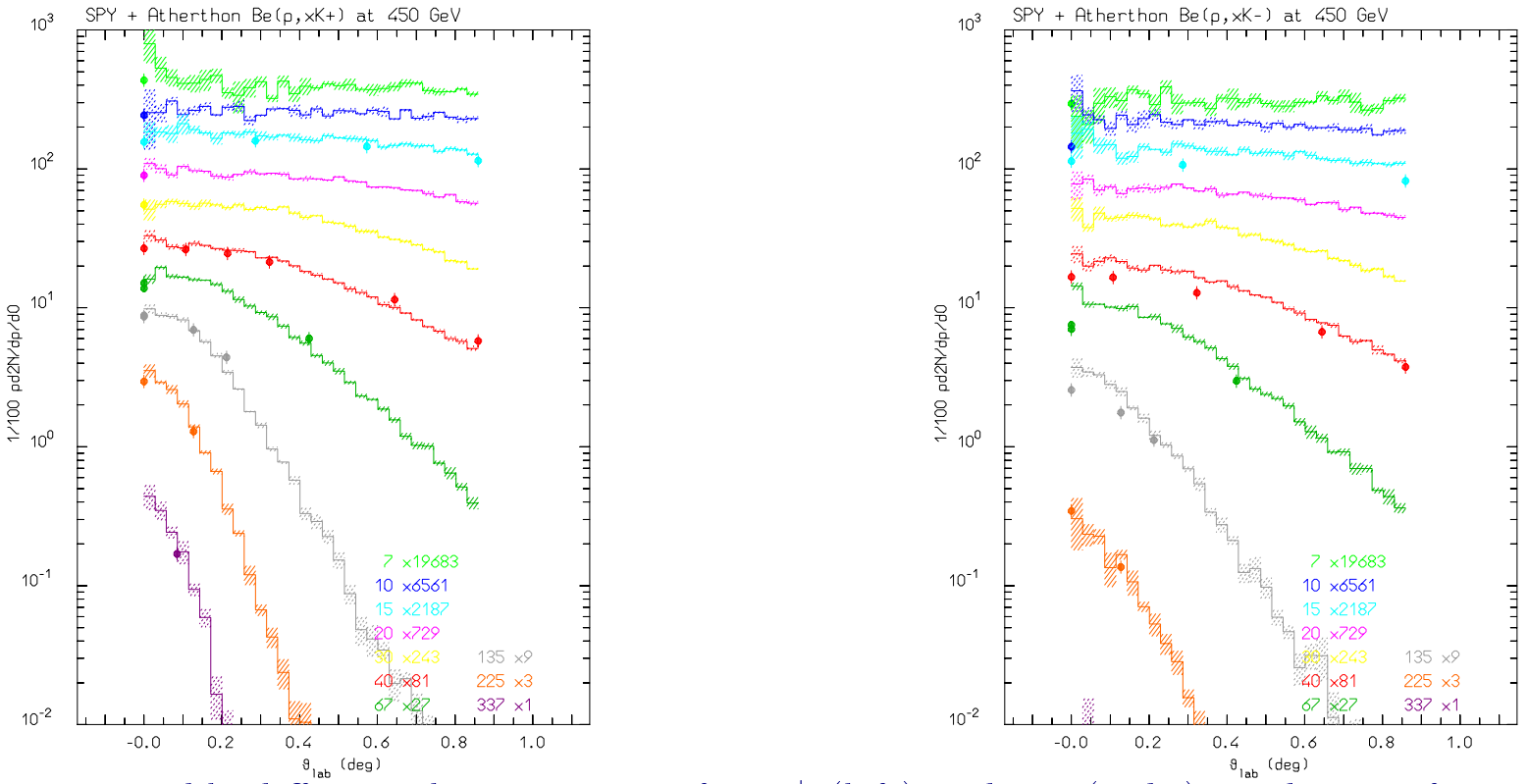

Double differential cross section for K^+ (left) and K^- (right) production for 450 GeV/c protons on a 10 cm thick Be target (data from H.W. Atherton CERN 80–07, G. Ambrosini et al. PL B425 208 (1988)).

Particle production in T9 Be target

($\Delta\Omega < 0.1$ **mSr E > 5 GeV**)

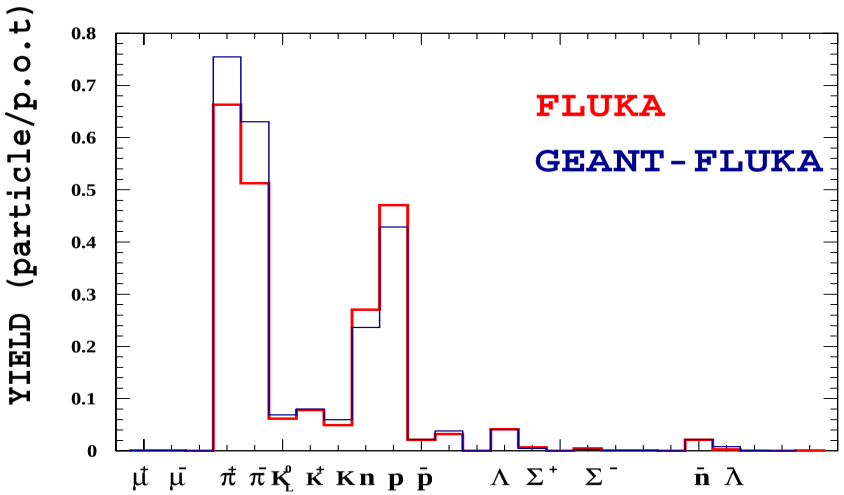

The particle spectrum at the end of T9 by FLUKA (full line) and GEANT-FLUKA (dashed line) with $P \geq 5$ GeV/c and $\theta \leq$ 10 mrad; neutrinos are not quoted.

Improvements: effect on WANF

Intensity, mean energy and relative abundances for ν fluxes at NOMAD fiducial area as calculated with the $FLUKA$ and $GEANT$-$FLUKA$ generator.

	Neutrino	intensity $[\nu/pot]$	$< E_\nu >$ $[GeV]$	relative abb.
FLUKA	ν_μ	1.11×10^{-2}	23.5	1.0
	$\overline{\nu}_\mu$		19.2	0.0627
	ν_e		37.1	0.0094
	$\overline{\nu}_e$		31.3	0.0024
GEANT-FLUKA	ν_μ	1.25×10^{-2}	23.5	1.0
	$\overline{\nu}_\mu$		23.1	0.0702
	ν_e		36.7	0.0092
	$\overline{\nu}_e$		34.2	0.0025

Complex benchmarks

Full cascade or neutron propagation benchmarks:

- The TIARA [1] neutron propagation experiment
- The TARC [2] experiment at CERN
- The Rösti [3] experiments at CERN
- The CEC [4] dosimetry facility at CERN
- Muon and hadron fluxes in the atmosphere
- Calorimeters [5]

[1] H.Nakashima et al. Nucl.Sci.Eng. **124** (1996); N. Nakao et al. Nucl.Sci.Eng. **124** (1996) 228
[2] H. Arnould et al., **PLB458** (1999) 167
[3] J.S.Russ et al, CERN/TIS **RP/89-02**, (1989); A.Fassò et al., CERN/TIS **RP/90-19**, (1990)
[4] A. Esposito et al, Rad. Prot. Dos. **76**, (1998) 135
[5] The ATLAS collaboration, NIM **387** (1997), 333 ; NIM **449** (2000), 461

Neutrino interactions in PEANUT: the *NUX-FLUKA* event generator

Authors: A. Ferrari (CERN/INFN), A. Rubbia (ETH Zurich), P.R. Sala (CERN/INFN)
Features:

- Full use of all sophisticated nuclear physics of PEANUT
- Quasielastic event generator built-in
- RES and DIS: nucleon density, position and Fermi motion via PEANUT $\rightarrow$ νN interaction via *NUX* (A.Rubbia, originally developed for NOMAD), $\rightarrow$ all secondaries propagated with PEANUT. Fully integrated one in the other in a single code $\rightarrow$ "correct" account for kinematical effects on cross section due to Fermi motion and for Pauli blocking

The comparison with NOMAD data are due to A. Bueno, A. Rubbia, ETH Zurich

The *NUX-FLUKA* event generator: comparison with NOMAD

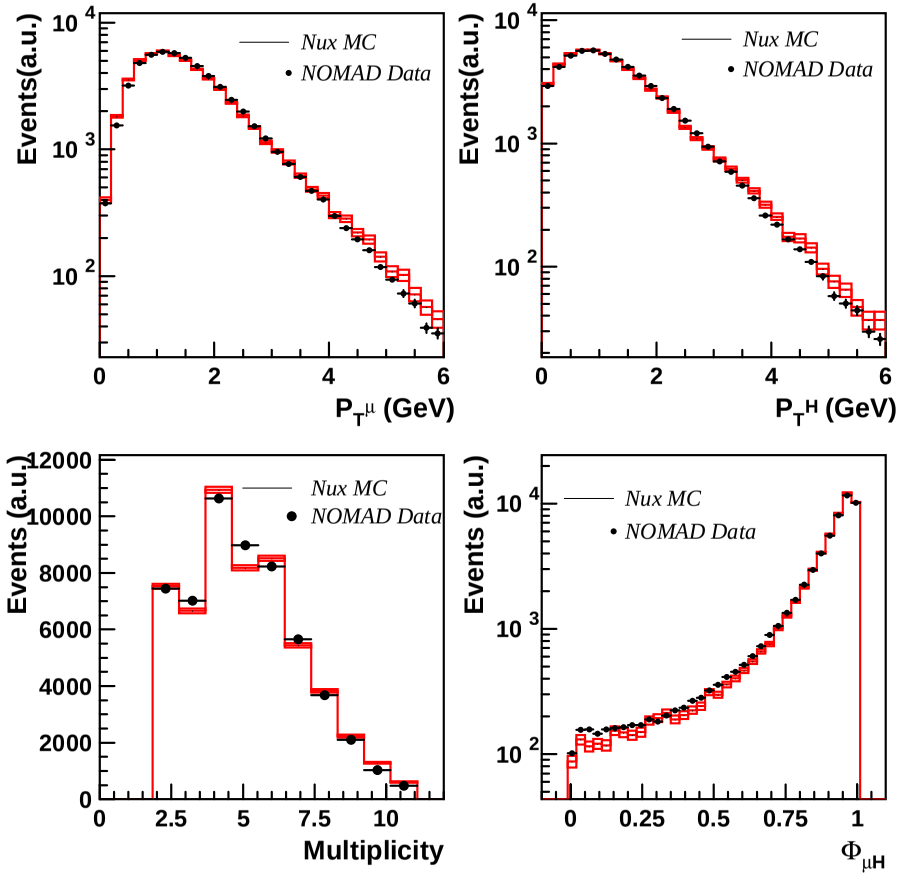

A 3-Dimensional Calculation of Atmospheric Neutrino Flux

G. Battistoni, A. Ferrari, P. Lipari, T. Montaruli, P.R. Sala, T. Rancati ,Astropart. Phys 12 (2000) 315

- based on FLUKA interaction and transport code
- 3D representation of Earth and atmosphere: 51 concentric shells of a mixture of N,O,Ar ($51 \equiv$ Earth surface, $1 \equiv 0.1 g/cm^2$) with Shibata "standard atmosphere" density profile
- primary particles sampled from continuous spectrum and injected at ~ 100 km altitude
- different geomagnetic models (applied at posteriori)
- all relevant physics included: energy losses, polarized decays ..

Comparison 3D/1D: angular distribution

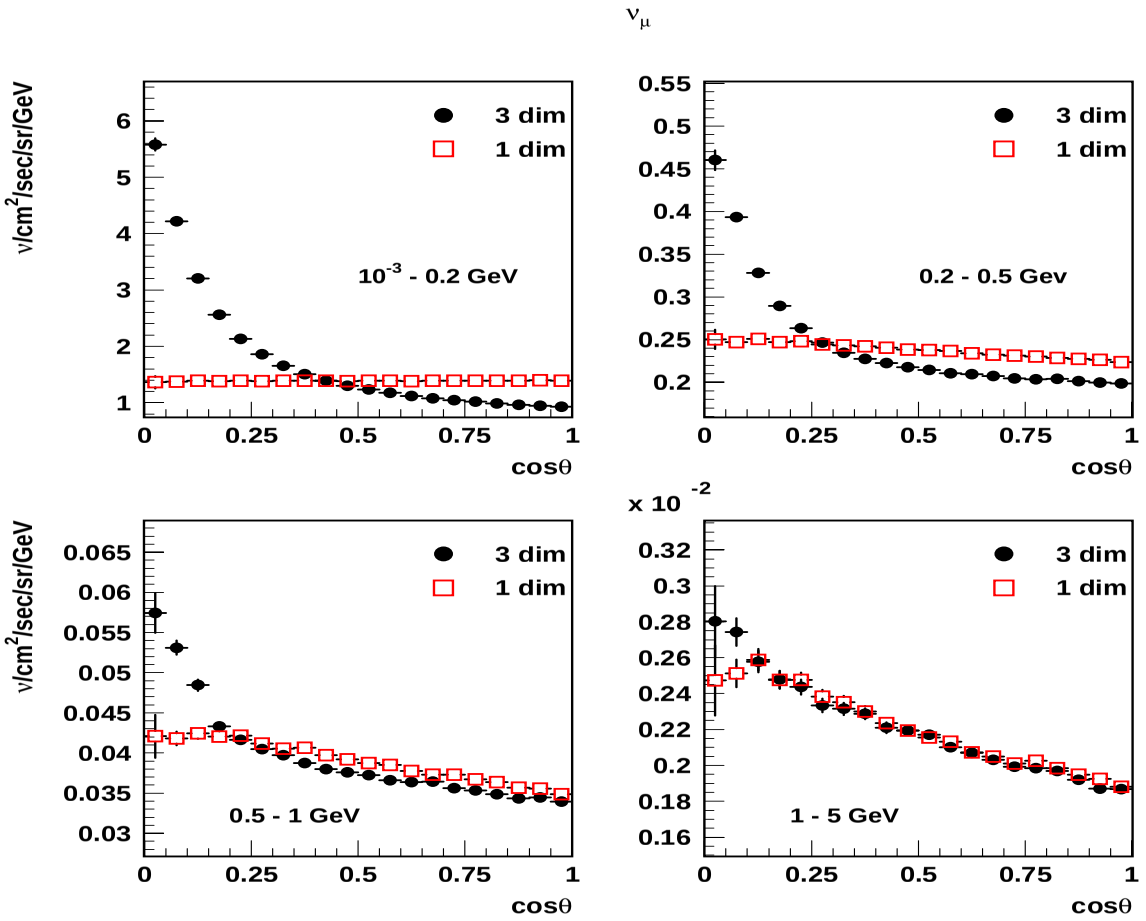

$\cos\theta$ distributions of ν_μ for 4 energy ranges for 1D/3D

Hadron/muon fluxes in the atmosphere

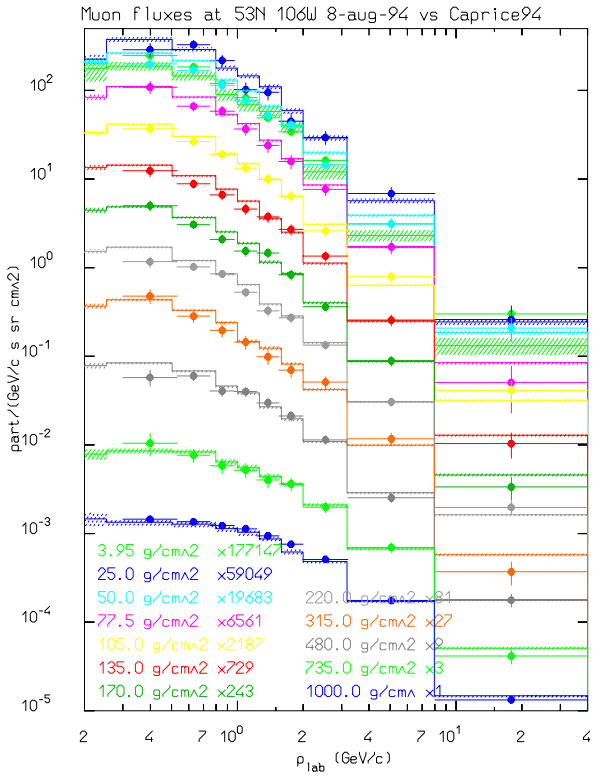

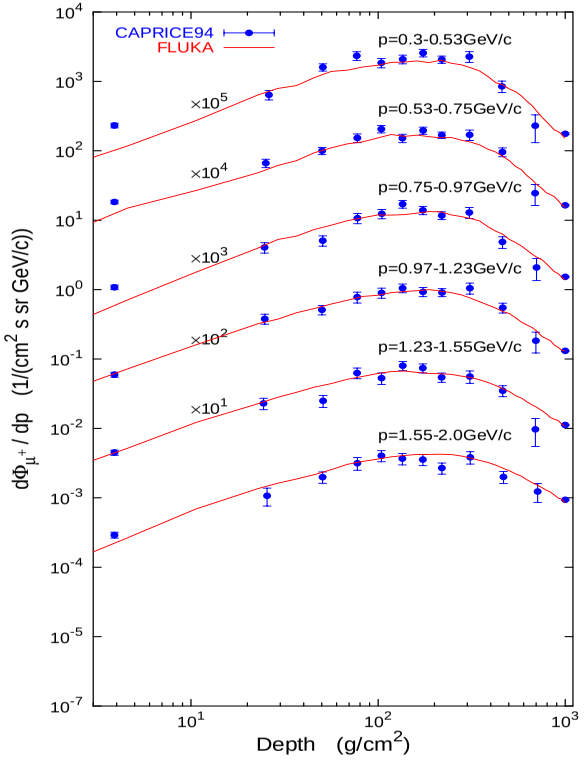

Muon fluxes at various atmospheric depths on 9-aug-94, compared with Caprice94 measurements.Right plot: courtesy of S. Roesler (SLAC)

FLUKA at CNGS

- Particle production in the target
- Neutrino spectra and rates at GS
- Energy absorption in the target
- Radiation damage/protection/activation (target, beam dump..)